

Direct spin accumulation quantification in ferromagnetic heterostructures using DC bias harmonic Hall measurement

Poh, Han Yin; Ang, Calvin Ching Ian; Gan, Weiliang; Lim, Gerard Joseph; Lew, Wen Siang

2021

Poh, H. Y., Ang, C. C. I., Gan, W., Lim, G. J. & Lew, W. S. (2021). Direct spin accumulation quantification in ferromagnetic heterostructures using DC bias harmonic Hall measurement. *Physical Review B*, 104, 224416-.
<https://dx.doi.org/10.1103/PhysRevB.104.224416>

<https://hdl.handle.net/10356/163173>

<https://doi.org/10.1103/PhysRevB.104.224416>

© 2021 American Physical Society. All rights reserved. This paper was published in *Physical Review B* and is made available with permission of American Physical Society.

Downloaded on 18 Jun 2024 03:22:44 SGT

Direct spin accumulation quantification in ferromagnetic heterostructures using DC bias harmonic Hall measurement

H. Y. Poh¹, C. C. I. Ang¹, W. L. Gan¹, , G.J. Lim¹, W.S. Lew^{1*}

¹*School of Physical and Mathematical Sciences, Nanyang Technological University,
21 Nanyang Link, Singapore 637371*

Abstract

We have shown that, by applying a DC bias during harmonic Hall measurement in Ta/Co/Pt structure with in-plane magnetic anisotropy, a net spin accumulation that results in an amplitude offset of the measured first harmonic Hall resistance in the Co layer, can be electrically quantified. A difference of the harmonic Hall resistance amplitudes when at opposite magnetisation states under a fixed DC bias was obtained, which gave direct measurements of spin accumulation up to 0.29% per kV/m of the local magnetization. The strength of both spin accumulation and damping-like efficiency was found to increase with larger Ta thicknesses, further verifying our experimental measurement that provides direct all-electrical quantification of spin accumulation.

* Corresponding author: wensiang@ntu.edu.sg

Introduction

The spin Hall effect (SHE) manifests as the conversion of electrical charge current flowing through a non magnetic material into a transverse spin current due to the effect of spin-dependent scattering [1–3]. The spin scattering leads to accumulation of spins along the lateral edges of the non magnetic layer. ~~The spin orientation at the HM interfaces are orthogonal to the direction of electron flow and interface normal [4].~~ If a heavy metal (HM) layer is used and is interfaced with a ferromagnetic (FM) layer, the accumulated spins diffuse from the HM layer into the FM layer. The injected spins exchange angular momentum with the local magnetization within the FM layer [5–11], inducing the spin orbit torque (SOT) effect. It is crucial to define a metric that describes and quantifies the spins accumulated within the FM layer, which determine the strength of the SOT. Characterisation of spin accumulation in the HM layer has been reported, for instance, using MOKE [3], X-ray magnetic circular dichroism (XMCD) [12,13] and Brillouin light scattering (BLS) measurement techniques [20]. However, due to the existence of spin backflow (SBF), where the spins are reflected back into the HM layer [14], and spin memory loss (SML), where the spin flips beyond the spin diffusion length [15,16], quantification of the spins that diffused into the FM layer, leading to field-like and damping-like fields, remains elusive. Therefore, a robust characterization technique that can directly quantify the spin accumulation in the FM layer has been a subject of continued pursuit in the effort of understanding the SOT mechanism.

In this Letter, we demonstrate direct electrical detection of spin accumulation in Co layer in a Ta/Co/Pt structure with in-plane magnetic anisotropy (IMA) using harmonic Hall measurement technique with a direct current (DC) bias. The inclusion of the DC bias results in an anomalous resistance originating from spin accumulation that is induced by the spin Hall

effect. The sign of this anomalous resistance is dependent on the accumulated spins being parallel or antiparallel to the local magnetization. A correlation between the quantified spin accumulation and the damping-like term was determined in a Ta thickness-dependent study of the anomalous first harmonic Hall resistance. Our spin quantification approach opens up a new avenue for direct measurement of spin accumulation in ferromagnetic layer via electrical method, which can potentially be more sensitive and accurate as compared to other techniques.

Main Text

The harmonic Hall measurement technique quantifies two mutually orthogonal components of the SOT: Damping-like field $\mathbf{H}_D = H_D \mathbf{m} \times \mathbf{p}$ and field-like field, $\mathbf{H}_F = H_F \mathbf{p}$, where \mathbf{p} is the polarized spin orientation of electrons [8,10,17–22]. In this technique, sweeping field and alternating current are applied to induce first and second harmonic Hall resistance, R_ω and $R_{2\omega}$ respectively. The R_ω provides information about the equilibrium magnetization direction and the $R_{2\omega}$ provides information about the SOT-induced small tilting of magnetization from the equilibrium via the planar Hall effect (PHE) and anomalous Hall effect (AHE) [20–24]. With the inclusion of spin accumulation that is induced by SHE by applied DC, it will result in the increase / decrease in PHE. The direction of the accumulated spin is dependent on the direction of the current flow and the sign of characteristic material spin Hall angle, θ_H . This can be described by $\hat{s} = (\hat{v} \times \hat{n}(\theta_H))$, where \hat{s} is the direction of the accumulated spin, \hat{v} is the direction of electron flow, and \hat{n} is the surface normal. Given the current flow in the $+\hat{x}$ -direction and structure with positive spin Hall angle (such as Pt), the electrons will then be polarized in the $\pm\hat{y}$ -direction towards the top/bottom interface. Therefore, we propose that the spin accumulation will manifest as a change in the planar Hall resistance in the \hat{y} -direction. The R_ω for an IMA structure can be expressed as $R_\omega = R_P \sin 2\phi$, where

R_p is planar Hall resistance which is proportional to $\mathbf{m}_x \cdot \mathbf{m}_y$ and ϕ is the azimuthal angle as shown in Fig 1a. Due to the accumulation of spins in the \hat{y} direction, the R_ω is given by:

$$R_\omega = r_p \left(m_x \cdot (m_y + \mathbf{s}) \right) \sin 2\phi \quad , \quad (1)$$

$$R_\omega = (R_p + \Delta R_p) \sin 2\phi \quad , \quad (2)$$

where r_p is the coefficient of planar Hall resistance, ΔR_p is the additional planar Hall resistance due to spin accumulation, and \mathbf{s} is the spin accumulation. The quantification of spin accumulation was measured by harmonic Hall measurement with DC bias, applying DC concurrently with the adiabatic AC along the Hall cross structure. The alignment of the magnetization in the \hat{y} -direction can be fixed by the external magnetic field, $\pm H_y$. The polarity of H_y will not affect ΔR_p since the polarity of accumulated spins are only dependent on the direction of current flow. By applying $\pm H_y$, the magnitudes of R_ω are expected to be different due to the direction of the accumulated spins. ΔR_p is obtained by summing up these values of $R_\omega(\pm H_y)$. This can be written as $\Delta R_p = \frac{R_\omega(+H_y) + R_\omega(-H_y)}{2}$. The spin accumulation is then determined by the ratio between ΔR_p and R_p . The applied DC bias is substantial to induced the thermoelectric effect, V_{TE} , however this effect is accounted for and found to be negligible. The sign V_{TE} is dependent on the magnetization ($\mathbf{m} \times \nabla T$) where ∇T is the temperature gradient due to Joule heating in the \hat{x} and \hat{z} -directions [25,26]. Since the sweeping field is in \hat{x} -direction, the first harmonic Hall voltage due to V_{TE} will be cancelled out due to the opposite signs of m_y . Hence, the V_{TE} has been eliminated in the quantification of the spin accumulation.

Methodology

Harmonic Hall measurements were carried out on Ta(2 nm)/Co(2 nm)/Pt(5 nm) Hall cross structure to characterize the SOT efficiency. The thin film stack was deposited by using DC magnetron sputtering, and subsequently patterned into a $5 \times 20 \mu\text{m}$ Hall cross structure using a combination of optical lithography and ion milling techniques. Vibrating sample magnetometer (VSM) measurement shows that the film stack has IMA with saturation magnetization, $M_s = 650 \pm 18 \text{ emu/cc}$ [27]. The harmonic Hall technique was used to obtain the R_ω and $R_{2\omega}$ with respect to the azimuthal angle of magnetization $\phi = \arctan \frac{H_y}{H_x}$, where H_x is the fixed external magnetic field of 600 Oe, and H_y is the sweeping magnetic field ranging from -4000 Oe to 4000 Oe . Uniform AC densities, j_{ac} ranging from $1 \times 10^{11} \text{ A/m}^2$ to $1.5 \times 10^{11} \text{ A/m}^2$ were applied in the \hat{x} -direction to obtain the damping-like efficiency. H_D is determined from $R_{2\omega}$ using [28]:

$$R_{2\omega} = R_A \frac{H_D}{2H_s} X + R_p \frac{H_F}{H_{x_{ext}}} (2X^4 - X^2), \quad (4)$$

where $X = \cos \phi$ and H_s is the saturation field. H_D is plotted against the electric field, \mathbf{E} as shown in Fig 2(b) and the electric field can be obtained by $\mathbf{E} = \rho_{xx} \mathbf{j}$, where ρ_{xx} is the resistivity of the structure, and \mathbf{j} is the uniform current density flowing into the structure. The dependence on electric field is preferred over uniform current density because the different resistivities of the layer will result in different current densities within the constituents of the trilayer. The uniform current density flowing into the trilayer will be less than the current density in Pt, hence resulting in overestimating the SOT efficiency. In addition, there are more than one source that generate SOT, it is experimentally impractical to isolate the individual SOT efficiency.

The SOT damping-like efficiency, ζ_{DL}^E can be calculated by $\zeta_{DL}^E = \frac{\mu_0 M_s t H_D}{E}$ [29], where μ_0 is the permeability of vacuum, and t is the thickness of the FM layer. The results for the $R_{2\omega}$ and ζ_{DL}^E for Ta/Co/Pt are shown in Fig. 2(c). The ζ_{DL}^E increased from $(20.05 \pm 0.07) \times 10^5 (\Omega\text{m})^{-1}$ to $(35.99 \pm 2.07) \times 10^5 (\Omega\text{m})^{-1}$ when the thickness of Ta is increased from 2 nm to 10 nm. This is because increasing the thickness of Ta will increase the percentage content of β -phase Ta which had been reported for higher contribution of SOT [30–32]. The magnitude of these ζ_{DL}^E correspond to approximately the effective spin Hall angle of 0.138 to 0.276 ($\theta_H^{eff} = \frac{2eM_s t H_D}{\hbar j}$) under the assumption of uniform current density injection through the trilayer structure which are comparable to various other reports [28,30,33–35].

Results

In order to quantify the spin accumulation in the FM layer, a uniform AC current density, $j_{ac} = 5.0 \times 10^{10} \text{ A/m}^2$ with a DC offset, $j_{dc} = 5.0 \times 10^{10} \text{ A/m}^2$ was injected through the trilayer structure in a longitudinal scheme with respect to the sweeping field. R_ω was measured under a sweeping magnetic field of $\pm 1000 \text{ Oe}$ in the \hat{x} -direction and a fixed magnetic field of 600 Oe in the \hat{y} -direction. As seen in Eq (2), the amplitude of R_ω determines the total planar Hall resistance, $(R_p + \Delta R_p)$. The experimental results show that R_p is measured to be $63.2 \text{ m}\Omega$ for zero DC bias meanwhile the total planar Hall resistances are $62.7 \text{ m}\Omega$ and $-64.0 \text{ m}\Omega$ for $+H_y$ and $-H_y$, respectively with DC offset. Therefore, we can conclude that the spin of the electrons are polarized in the $-\hat{y}$ -direction in the FM layer. With the presence of DC bias, the polarized spins are aligned parallel (antiparallel) to the localized magnetization of the FM, leading to an increase (decrease) in total magnetization as illustrated in Fig 1(b). Without an applied DC ($j_{DC} = 0$), there will be no net accumulated spin. Hence, the amplitude of the R_ω between $+H_y$ and $-H_y$ is expected to be the same. The ΔR_p is

obtained by summing the amplitude of R_ω for $\pm H_y$. A linear trend in ΔR_p is observed from the sweeping j_{DC} from 1×10^{10} A/m² to 5×10^{10} A/m². Thus, a linear fit is used to determine the rate of change of ΔR_p per electric field. From the gradient of the linear fit, the spin accumulation is calculated by $\mathbf{s} = \frac{1}{R_p} \frac{d\Delta R_p}{dE}$.

To both confirm that the SHE is the dominant source resulting in spin accumulation, and that an increase in spin accumulation, and that an increase in spin accumulation would lead to a larger ΔR_p , measurement were performed on samples with Ta thickness ranging from 2 nm to 10 nm. The measurement results of spin accumulation in the Co layer with varying Ta thickness are shown in Fig. 4. Factoring in the M_s of the Hall structure, the obtained spin accumulation results are $1.19 \times 10^{17} \mu_B/cm^3$ per V/m and $2.05 \times 10^{17} \mu_B/cm^3$ per V/m, for Ta = 2 nm and Ta = 10 nm, respectively. In addition, a similar trend of spin accumulation and the ζ_{DL}^E with Ta thickness in Ta/Co/Pt is observed, as shown in Fig 4. The Rashba effect is an interfacial effect, which is independent of the HM thickness whereas SHE is a bulk effect which is dependent on the HM thickness. These results further affirm the dominance of the spin Hall effect in our stack structures, which is the cause of spin accumulation building up in the FM layer. To quantify the degree of influence in spin accumulation on the FM layer, the measured spin accumulation is normalized to the saturation magnetization of the FM layer and a value of 0.29% per kV/m in Co for Ta(10)/Co(2)/Pt(5) is obtained.

The measurement was repeated on another IMA sample of Ti(2)/Co(2)/Pt(5) with Ti ranging from 2 nm to 10 nm. Since Ti was reported to have low damping-like term, it will be intriguing to determine how the spin accumulation changes with the damping-like efficiency. The results of the spin accumulation and damping-like efficiency are shown in Fig 4. Spin

accumulation of $2.09 \times 10^{16} \mu_B/cm^3$ per V/m was obtained for the Ti(2)/Co(2)/Pt(5) sample. The measured spin accumulation from Ti, \mathbf{s}_{Ti} is lower than spin accumulation from Ta, \mathbf{s}_{Ta} . This further shows that spin accumulation is proportional to the damping-like efficiency.

In conclusion, current-induced spin accumulation in Ta/Co/Pt and Ti/Co/Pt structures have been quantified using the harmonic Hall measurement technique with DC bias. Our experiments show that the spin accumulation is approximately 0.29% per kV/m of the local magnetization for 10 nm Ta. Our results demonstrate that, besides the conventional SOT measurement, spin accumulation can also be quantified using harmonic Hall technique. The ratio of the spin accumulation over the applied electric field shows similar trend with damping-like efficiency as the thickness of HM increases. Hence, the ratio can be used to evaluate the efficiency of a HM in converting electric current to spin current. This provides an all-electrical alternative to determine spin accumulation by utilizing the easily accessible harmonic Hall characterization technique.

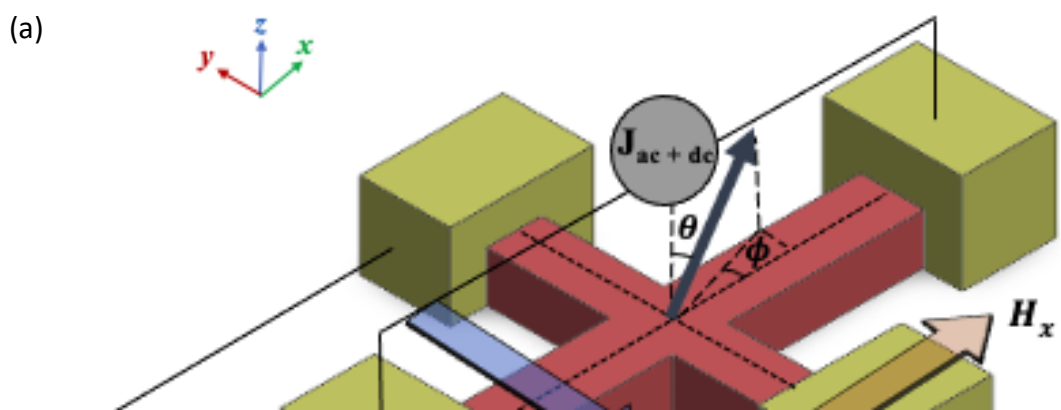


Figure 1: (a) Schematic of DC bias harmonic Hall setup in the longitudinal configuration. (b) Schematic of the spin accumulation in the FM/HM structure with in-plane anisotropy. Spins are accumulated in the $+\hat{y}$ direction in the FM when injected electron is in the direction of $+\hat{x}$. Local magnetization, \mathbf{m} follows the direction of external field, H_y . Amplitude of first Harmonics resistance, R_ω will increase (decrease) if spin accumulations, s , are parallel (antiparallel) to the local magnetization of the FM layer as described in Eq (2).

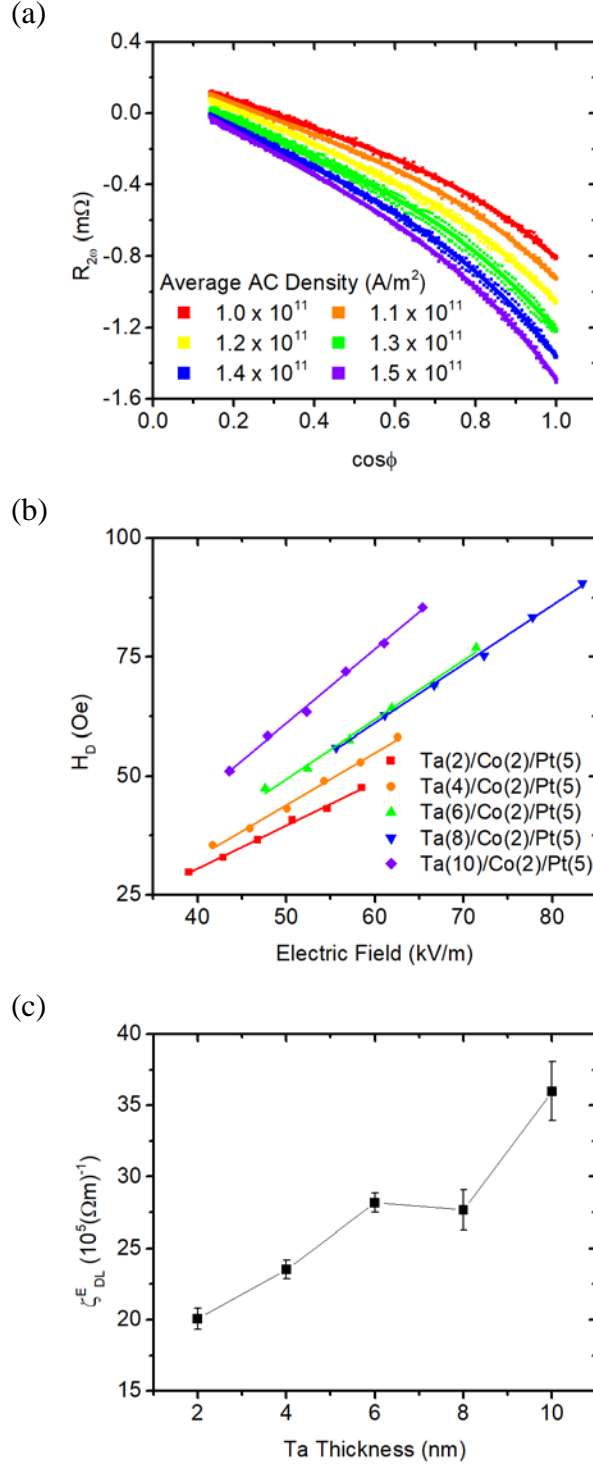


Figure 2: (a) $R_{2\omega}$ as a function of $\cos\phi$, for average current density ranging from $1 - 1.5 \times 10^{10} \text{ A/m}^2$. Graph of $AX + B(2X^4 - X^2)$ is fitted to the data. (b) H_D as a function of electric field for various Ta thicknesses ranging from 2 nm to 10 nm. (c) ζ_{DL}^E as a function of Ta thickness.

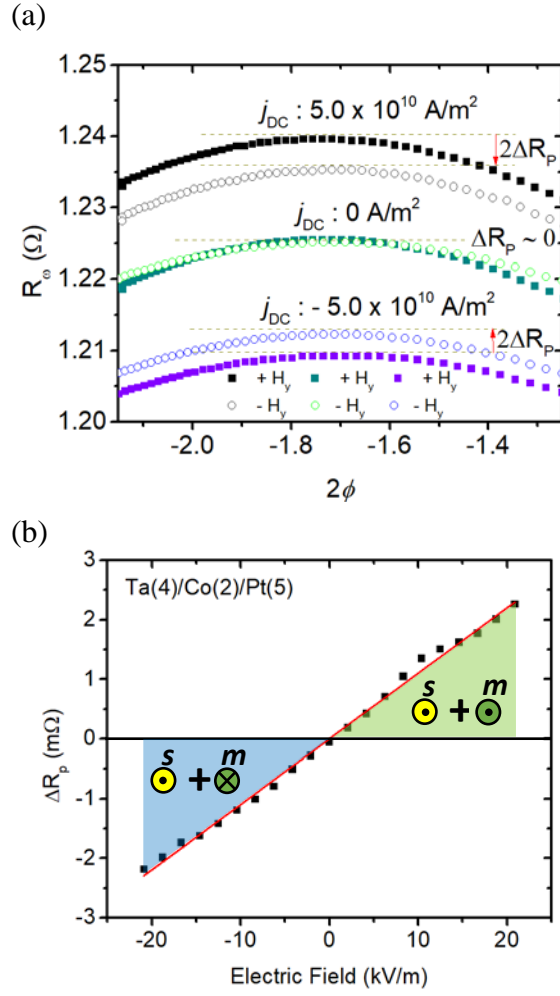


Figure 3: (a) R_ω for $+H_y$ (solid square) and $-H_y$ (open circle). Offsets have been applied to the R_ω for better clarity. R_ω for $-H_y$ is flipped for clearer comparison. Spin accumulation is parallel (antiparallel) to $+H_y$ ($-H_y$), leading to a higher amplitude in the R_ω at the current density of $j_{DC} = 5.0 \times 10^{10} \text{ A/m}^2$. (b) Amplitude of ΔR_P with respect to electric field. The slope of ΔR_P over electric field is $0.11 \text{ m}\Omega$ per kV/m .

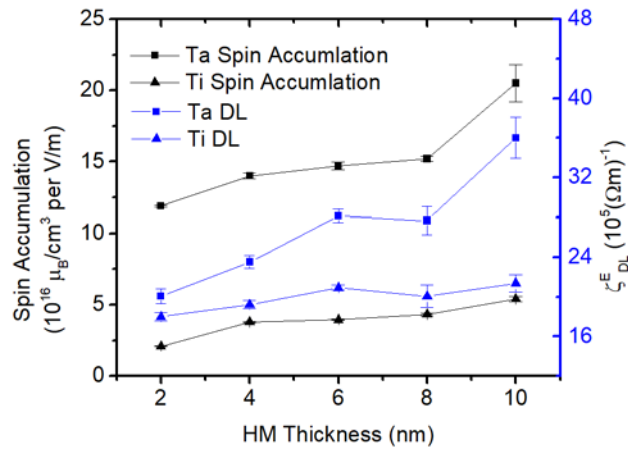


Figure 4: Spin accumulation of Ta (black square) and Ti (black triangle), and DL efficiency of Ta (blue square) and Ti (black triangle) with various HM thickness ranging from 2 nm to 10 nm.

Reference

- [1] J. Sinova, S. O. Valenzuela, J. Wunderlich, C. H. Back, and T. Jungwirth, *Spin Hall Effects*, Rev. Mod. Phys. **87**, 1213 (2015).
- [2] S. Murakami and N. Nagaosa, *Spin Hall Effect*, Compr. Semicond. Sci. Technol. **1–6**, 222 (2011).
- [3] C. Stamm, C. Murer, M. Berritta, J. Feng, M. Gabureac, P. M. Oppeneer, and P. Gambardella, *Magneto-Optical Detection of the Spin Hall Effect in Pt and W Thin Films*, Phys. Rev. Lett. **119**, 1 (2017).
- [4] F. Auvray, J. Puebla, M. Xu, B. Rana, D. Hashizume, and Y. Otani, *Spin Accumulation at Nonmagnetic Interface Induced by Direct Rashba–Edelstein Effect*, J. Mater. Sci. Mater. Electron. **29**, 15664 (2018).
- [5] S. O. Valenzuela and M. Tinkham, *Direct Electronic Measurement of the Spin Hall Effect*, Nature **442**, 176 (2006).
- [6] M. I. Dyakonov and V. I. Perel, *Current-Induced Spin Orientation of Electrons in Semiconductors*, Phys. Lett. A **35**, 459 (1971).
- [7] I. M. Miron, K. Garello, G. Gaudin, P. J. Zermatten, M. V. Costache, S. Auffret, S. Bandiera, B. Rodmacq, A. Schuhl, and P. Gambardella, *Perpendicular Switching of a Single Ferromagnetic Layer Induced by In-Plane Current Injection*, Nature **476**, 189 (2011).
- [8] S. Emori, U. Bauer, S. M. Ahn, E. Martinez, and G. S. D. Beach, *Current-Driven Dynamics of Chiral Ferromagnetic Domain Walls*, Nat. Mater. **12**, 611 (2013).
- [9] X. Fan, H. Celik, J. Wu, C. Ni, K. J. Lee, V. O. Lorenz, and J. Q. Xiao, *Quantifying Interface and Bulk Contributions to Spin-Orbit Torque in Magnetic Bilayers*, Nat. Commun. **5**, (2014).
- [10] T. D. Skinner, K. Olejník, L. K. Cunningham, H. Kurebayashi, R. P. Campion, B. L. Gallagher, T. Jungwirth, and A. J. Ferguson, *Complementary Spin-Hall and Inverse Spin-Galvanic Effect Torques in a Ferromagnet/Semiconductor Bilayer*, Nat. Commun. **6**, 4 (2015).
- [11] A. Manchon and S. Zhang, *Theory of Spin Torque Due to Spin-Orbit Coupling*, Phys. Rev. B - Condens. Matter Mater. Phys. **79**, 1 (2009).
- [12] R. Kukreja, S. Bonetti, Z. Chen, D. Backes, Y. Acremann, J. A. Katine, A. D. Kent, H. A. Dürr, H. Ohldag, and J. Stöhr, *X-Ray Detection of Transient Magnetic Moments*

- Induced by a Spin Current in Cu*, Phys. Rev. Lett. **115**, 1 (2015).
- [13] C. Stamm, C. Murer, Y. Acremann, M. Baumgartner, R. Gort, S. Daster, A. Kleibert, K. Garello, J. Feng, M. Gabureac, Z. Chen, J. Stohr, and P. Gambardella, *X-Ray Spectroscopy of Current-Induced Spin-Orbit Torques and Spin Accumulation in Pt/3d-Transition-Metal Bilayers*, Phys. Rev. B **100**, 1 (2019).
- [14] K. Hashimoto, G. Tatara, and C. Uchiyama, *Spin Backflow: A Non-Markovian Effect on Spin Pumping*, Phys. Rev. B **99**, 205304 (2019).
- [15] K. Chen and S. Zhang, *Spin Pumping in the Presence of Spin-Orbit Coupling*, Phys. Rev. Lett. **114**, 1 (2015).
- [16] J. Borge and I. V. Tokatly, *Ballistic Spin Transport in the Presence of Interfaces with Strong Spin-Orbit Coupling*, Phys. Rev. B **96**, 1 (2017).
- [17] I. M. Miron, G. Gaudin, S. Auffret, B. Rodmacq, A. Schuhl, S. Pizzini, J. Vogel, and P. Gambardella, *Current-Driven Spin Torque Induced by the Rashba Effect in a Ferromagnetic Metal Layer*, Nat. Mater. **9**, 230 (2010).
- [18] K. Garello, I. M. Miron, C. O. Avci, F. Freimuth, Y. Mokrousov, S. Blugel, S. Auffret, O. Boulle, G. Gaudin, and P. Gambardella, *Symmetry and Magnitude of Spin-Orbit Torques in Ferromagnetic Heterostructures*, Nat. Nanotechnol. **8**, 587 (2013).
- [19] X. Wang and A. Manchon, *Diffusive Spin Dynamics in Ferromagnetic Thin Films with a Rashba Interaction*, Phys. Rev. Lett. **108**, 1 (2012).
- [20] J. Kim, J. Sinha, M. Hayashi, M. Yamanouchi, S. Fukami, T. Suzuki, S. Mitani, and H. Ohno, *Layer Thickness Dependence of the Current-Induced Effective Field Vector in Ta/CoFeB/MgO*, Nat. Mater. **12**, 240 (2013).
- [21] M. Jamali, K. Narayanapillai, X. Qiu, L. M. Loong, A. Manchon, and H. Yang, *Spin-Orbit Torques in Co/Pd Multilayer Nanowires*, Phys. Rev. Lett. **111**, 1 (2013).
- [22] M. Hayashi, J. Kim, M. Yamanouchi, and H. Ohno, *Quantitative Characterization of the Spin-Orbit Torque Using Harmonic Hall Voltage Measurements*, Phys. Rev. B - Condens. Matter Mater. Phys. **89**, 1 (2014).
- [23] P. P. J. Haazen, E. Mure, J. H. Franken, R. Lavrijsen, H. J. M. Swagten, and B. Koopmans, *Domain Wall Depinning Governed by the Spin Hall Effect*, Nat. Mater. **12**, 299 (2013).
- [24] X. Qiu, W. Legrand, P. He, Y. Wu, J. Yu, R. Ramaswamy, A. Manchon, and H. Yang, *Enhanced Spin-Orbit Torque via Modulation of Spin Current Absorption*, Phys. Rev.

- Lett. **117**, 1 (2016).
- [25] E. S. Park, D. K. Lee, B. C. Min, and K. J. Lee, *Elimination of Thermoelectric Artifacts in the Harmonic Hall Measurement of Spin-Orbit Torque*, Phys. Rev. B **100**, 1 (2019).
- [26] H. Yang, H. Chen, M. Tang, S. Hu, and X. Qiu, *Characterization of Spin-Orbit Torque and Thermoelectric Effects via Coherent Magnetization Rotation*, Phys. Rev. B **102**, 1 (2020).
- [27] Q. Y. Wong, C. Murapaka, W. C. Law, W. L. Gan, G. J. Lim, and W. S. Lew, *Enhanced Spin-Orbit Torques in Rare-Earth Pt/[Co/Ni]₂/Co/Tb Systems*, Phys. Rev. Appl. **11**, 1 (2019).
- [28] F. Luo, S. Goolaup, W. C. Law, S. Li, F. Tan, C. Engel, T. Zhou, and W. S. Lew, *Simultaneous Determination of Effective Spin-Orbit Torque Fields in Magnetic Structures with in-Plane Anisotropy*, Phys. Rev. B **95**, 1 (2017).
- [29] L. Zhu, D. C. Ralph, and R. A. Buhrman, *Enhancement of Spin Transparency by Interfacial Alloying*, Phys. Rev. B **99**, 1 (2019).
- [30] S. Woo, M. Mann, A. J. Tan, L. Carretta, and G. S. D. Beach, *Enhanced Spin-Orbit Torques in Pt/Co/Ta Heterostructures*, Appl. Phys. Lett. **105**, 212404 (2016).
- [31] L. Liu, C. F. Pai, Y. Li, H. W. Tseng, D. C. Ralph, and R. A. Buhrman, *Spin-Torque Switching with the Giant Spin Hall Effect of Tantalum*, Science (80-.). **336**, 555 (2012).
- [32] G. Allen, S. Manipatruni, D. E. Nikonov, M. Doczy, and I. A. Young, *Experimental Demonstration of the Coexistence of Spin Hall and Rashba Effects in β -Tantalum/Ferromagnet Bilayers*, Phys. Rev. B - Condens. Matter Mater. Phys. **91**, 1 (2015).
- [33] C. Hahn, G. De Loubens, O. Klein, M. Viret, V. V. Naletov, and J. Ben Youssef, *Comparative Measurements of Inverse Spin Hall Effects and Magnetoresistance in YIG/Pt and YIG/Ta*, Phys. Rev. B - Condens. Matter Mater. Phys. **87**, 1 (2013).
- [34] F. Luo, Q. Y. Wong, S. Li, F. Tan, G. J. Lim, X. Wang, and W. S. Lew, *Dependence of Spin-Orbit Torque Effective Fields on Magnetization Uniformity in Ta/Co/Pt Structure*, Sci. Rep. **9**, 0 (2019).
- [35] S. Woo, M. Mann, A. Tan, L. Carreta, and G. Beach, *Characterization of Spin-Orbit*

Torques in Pt/Co/Ta Structures, 1 (2015).